

## **Study the Effect of the Magnetic Field on the Electrical Characteristics of the Glow Discharge**

**M. A. Hassouba<sup>\*1,2</sup> and N. Dawood<sup>2</sup>**

<sup>1</sup> *Physics Dept., Faculty of Science, Benha Univ., Egypt.*

<sup>2</sup> *Applied Physics Dept., Faculty of Applied Science, Taibah Univ., KSA*

---

### **ABSTRACT**

*Low-density plasma is generated in a cylindrical DC magnetron discharge tube. The radial and axial distributions of the magnetic field strengths are drawn. The discharge current and voltage ( $I_a$ - $V_a$ ) characteristic curves of the glow discharge have been measured for Ar and He gases pressures. The effect of the applied magnetic field on the ( $I_a$ - $V_a$ ) characteristic curves and on the cathode fall thickness is discussed. The breakdown potentials ( $V_B$ ) of the discharge are lower when the magnetic field is applied.*

**Key words:-** Glow discharge, cathode fall thickness, Larmor radius.

---

### **INTRODUCTION**

Glow discharges are used in a range of application fields: in the microelectronics industry for thin film deposition and plasma etching, as plasma display panels, as metal vapor ion lasers, as fluorescent lamps, and also in analytical chemistry [1].

Glow discharge is characterized by the appearance of several luminous zones and by a constant potential difference between the two electrodes independent of the discharge current. The relative size of these zones varies with gas pressure and the distance between the two electrodes and the glow intensity depends on the number density and energy of the excited electrons [2].

The main effect of the magnetic field on the glow discharge is the cause the electrons and ions to move no longer in straight lines but to orbits around the magnetic field lines in circular orbits of radius equal to:

$$r_e = mv = eB$$

Where  $v$  is the electron velocity,  $B$  is the magnetic field strength and  $e$ ,  $m$  are the charge and mass of electrons. This radius is called the Larmor or gyro radius. The particle motion across the magnetic field is thus greatly restricted although the motion along the field is essentially as before [3].

Clearly the electron Larmor radius is smaller than the ion radius (for comparable  $T_e$  and  $T_i$ ) by the factor:

$$(m_e/m_i)^{1/2}$$

As a result, the electrons are more strongly affected by the magnetic field than the ions [3].

Recently [4-7], some correlative works are developed to investigate the effects of magnetic field on the structure of the plasma sheath.

Zou et al.[4] has shown that the characteristics of the plasma sheath in an oblique magnetic field cannot be ignored compared to the electrostatic field. They investigated the structure of the plasma sheath in an external magnetic field without considering the effect of collision. It is shown that considering an external magnetic field makes some fluctuations in ion flow velocity and density distribution. These fluctuations strongly depend on the component of magnetic field in depth direction; bigger the angle between the magnetic field and depth direction, more obvious the fluctuations.

In the present work, the distribution of the magnetic field strengths in the radial direction of the cathode electrode and the axial distribution between the two electrodes are drawn. Also, the ( $I_a$ - $V_a$ ) characteristic curves of the glow discharge have been measured for Ar and He gases with and without magnetic field. The cathode fall thickness is measured at different gas pressure.

## MATERIALS AND METHODS

A stationary DC-glow discharge was generated between two electrodes of metallic discs of about 5 cm in diameter. The anode was made of copper and the cathode of aluminum or another metal according to the sputtering purposes. The two electrodes were placed inside the metallic chamber of 15 cm diameter which was evacuated down to about  $10^{-5}$  mbar using a large rotary pump and two stages of diffusion pumps. Pure Argon and Helium gases were introduced into the system via a needle valve. The discharge current ( $I_a$ ) was varied between 4 and 30 mA and the gas pressure ( $P$ ) was in the range 0.5 to 6 mbar for each of the two gases. The device was operated using discharge voltage ( $V_a$ ) varied between 200 to 1000 V DC, whereas the current density was between 2 and 15 mA/m<sup>2</sup>.

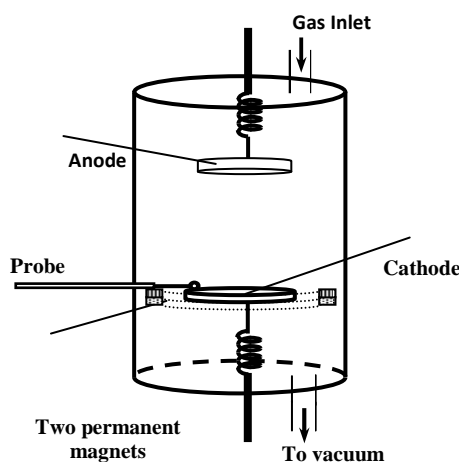
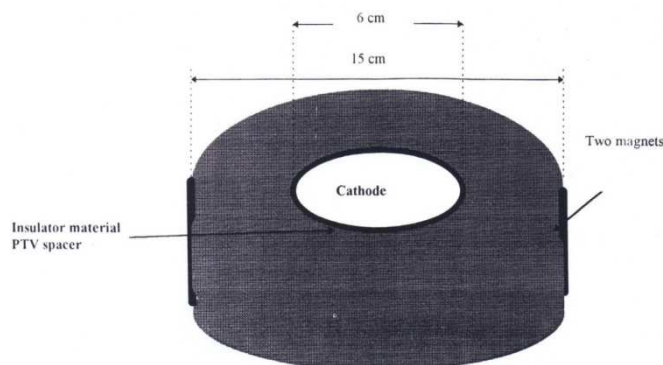


Figure (1) schematic drawing of the apparatus used in this study

Two permanent circular magnets are placed around the cathode surface to produce the magnetic field. The geometry and the dimension of the magnet is shown in Fig. (2).



**Fig. (2) The geometry and the dimension of the magnet**

The MG-4D Hall probe, which is a fully portable hand-held Hall effect gauss meter, is used to measure the magnetic field strengths  $B$ .

A cylindrical single probe 1.0-mm diameter and length 0.5 mm, molybdenum wire is used to measure the axial potential distribution of the discharge.

## RESULTS AND DISCUSSION

### 3-1. DISTRIBUTION OF THE MAGNETIC FIELD STRENGTHS.

Figure (3) shows the radial distribution of the magnetic field strength  $B$  measured by a Hall probe which moving along the cathode surface from one edge to the other. The magnetic field strength  $B$  is maximum at the two cathode edges and is a minimum at the center of the cathode where the magnetic field strength  $B$  is very weak.

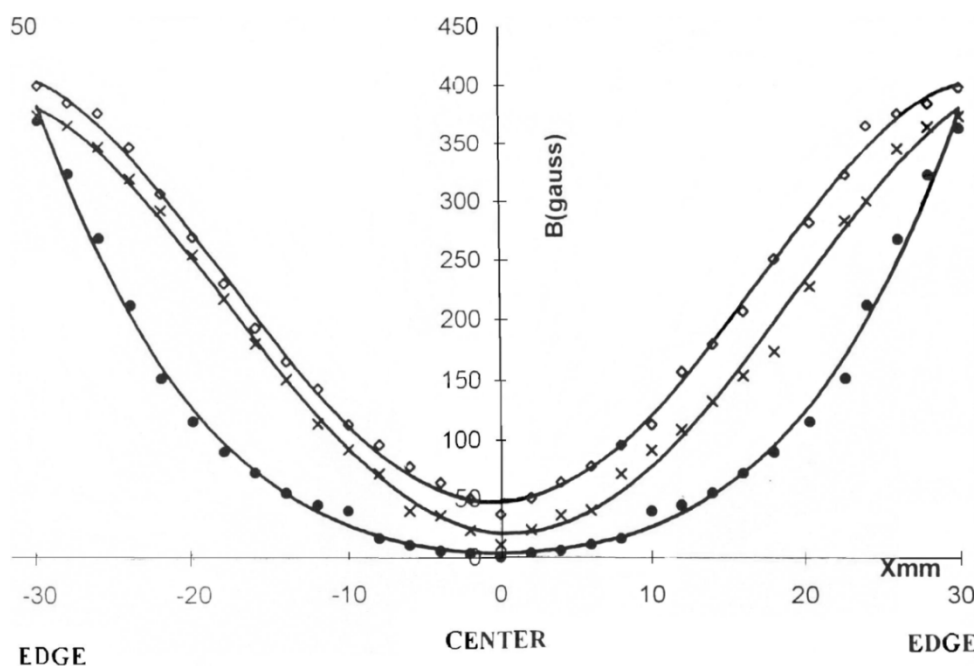


**Fig. (3) The radial distribution of the magnetic field Strength**

On the other hand, Fig. (4) shows the axial distribution along the discharge tube when the Hall probe moved from the edge of the cathode to the edge of the anode. The magnetic field strength  $B$  is maximum at the edge of the cathode fall region then it decrease to the edge of the anode passing through the negative glow region.

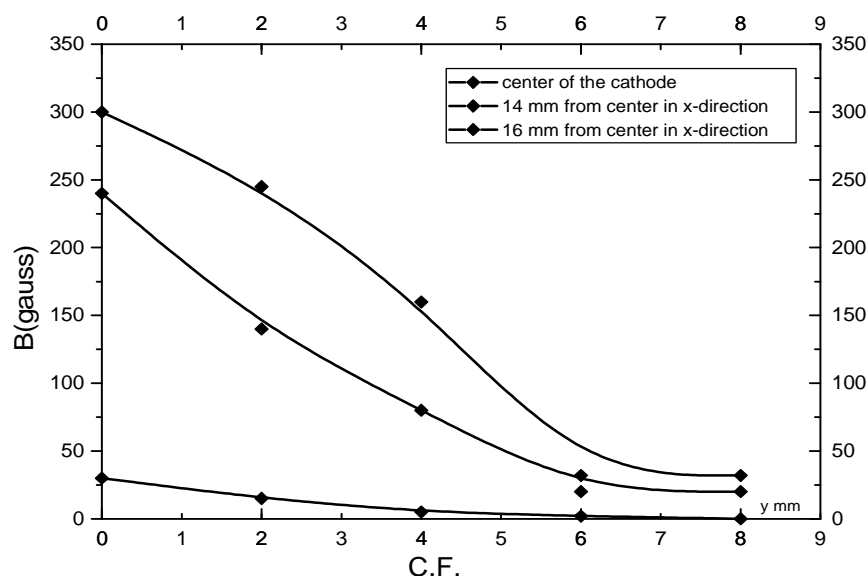


Fig. (4) The axial distribution of the magnetic field along the discharge tube

### 3-2. THE ( $I_a$ - $V_a$ ) CHARACTERISTIC CURVES OF THE GLOW DISCHARGE.

Figure (5) shows the ( $I_a$ - $V_a$ ) characteristic curves of the Argon gas discharge in the pressure range of (0.53 - 4.0) mbar, whereas the distance between the two electrodes was fixed at (3.2 cm). This distance is long enough for the existence of the different regions of the glow discharge [2]. The upper limits of  $I_a$  and  $V_a$  are limited by the power of the DC power supply. Since at low pressure, the probability of electron ionizing collisions with atoms will decrease (i.e. the mean free path will increase) large values of the discharge voltage will be required to maintain the discharge and a small discharge current  $I_a$  is expected. At high pressures number of electron – atom ionizing collisions increases. Thus, more electrons and positive ions are produced and consequently, the discharge current is increased at the same voltage [8].

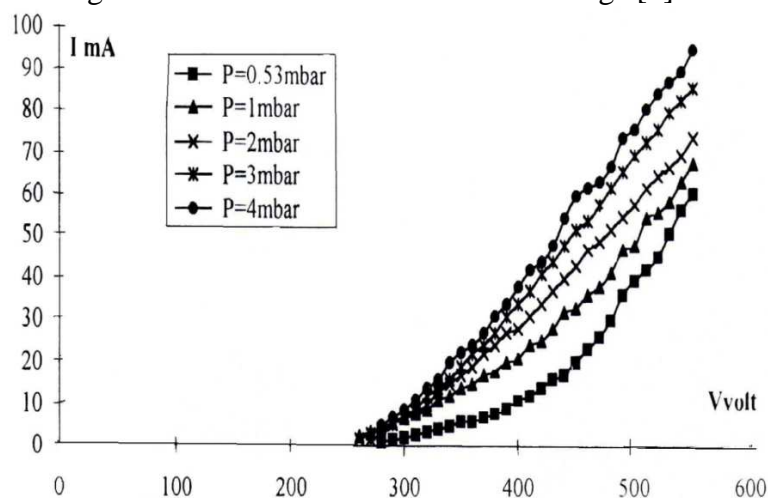


Fig. (5) The ( $I_a$ - $V_a$ ) characteristic curves of the Argon gas discharge at different pressures, when the distance between the two electrodes was fixed at (3.2 cm)

On the other hand, the ( $I_a$ - $V_a$ ) characteristic curves of Argon gas at pressures of (0.53, 1 2, 3, and 4 mbar) when the external magnetic field is applied are shown in Fig (6). The curves are similar to those without magnetic field, although the breakdown potentials of the discharge were lower as shown Fig. (7).

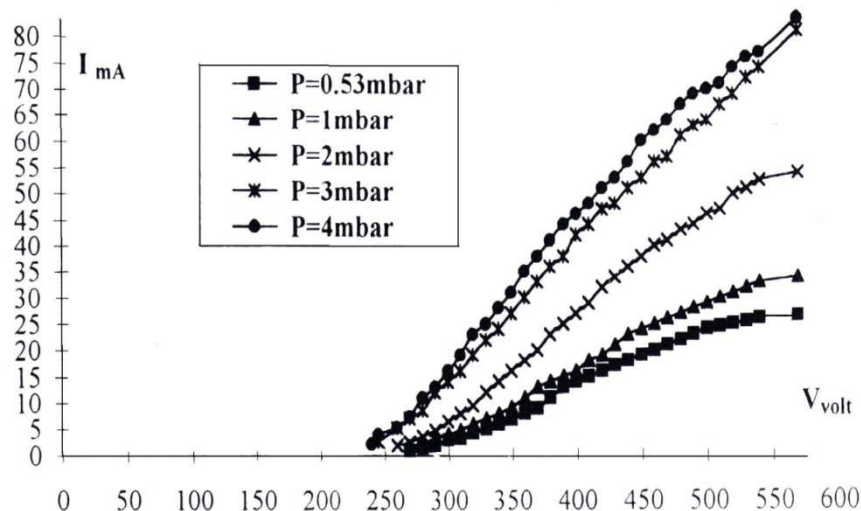


Fig. (6) The ( $I_a$ - $V_a$ ) characteristic curves of Argon gas at different pressures when applied the external magnetic field

The breakdown potentials ( $V_B$ ) of the discharge are lower when the magnetic field is applied, this can be explained as follows:- the current density can be increased by the magnetic field , due to the effective increase in the gas pressure . This is related to the fact that the presence of the magnetic field increases the apparent gas pressure and thus decreasing the mean free path, hence more excitation and ionization processes occurred and consequently the breakdown potential decreased as shown in Fig. (7).

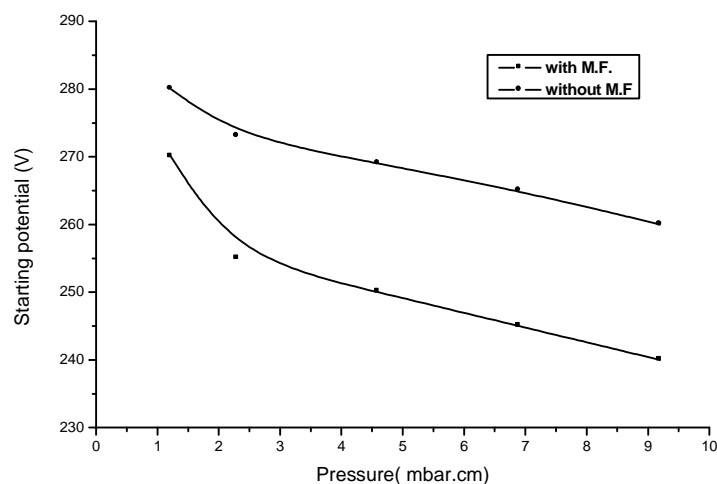


Fig. (7) The breakdown potentials measurements with and without the magnetic for the Argon gas at different pressures.

The decrease of the discharge voltage in the magnetic field results from the increase in the number of collisions between the primary electrons and neutral gas atoms. The effects of the magnetic field are qualitatively considered to be effective pressure  $p_e$ , given by [9]

$$p_e/p = \{1 + (\omega\tau)^2\}^{1/2}$$

Where  $\omega$  is the cyclotron frequency of the electron and  $\tau$  is the mean free time of the electron. Since [9]

$$\omega = \frac{eB}{m}$$

and

$$\tau = \frac{\lambda_o}{p \left[ 2 \left( \frac{e}{m} \right) V_o^{0.5} \right]}$$

$$\omega\tau = \frac{\lambda_o B \left( \frac{e}{m} \right)^{1/2}}{\sqrt{2} p V_o^{1/2}}$$

Where  $\lambda_o$  is the mean free path of the electron at 1 torr, B is the strength of the magnetic field,  $(e/m)$  is the specific charge of the electron and  $V_o$  is the acceleration voltage for the electron. Taking  $B = 100$  G,  $p = 1$  torr (Ar),  $V_o = 100$  V and  $\lambda_o = 0.05$  cm, we obtain  $\omega\tau = 5 \times 10^3$ , and  $p_e = 0.05$  torr.

Values of the discharge current in the presence of the magnetic field for Argon are smaller to those in the absence of the magnetic field. Thus, slopes of the  $(I_a-V_a)$  curves in the presence of the magnetic field are smaller than those in the absence of magnetic field, (i.e. the resistance of the discharge is larger when no magnetic field is applied).

For Helium discharge, similar  $(I_a-V_a)$  characteristic curve are obtained in the gas pressure range of (0.53-4.0) mbar as shown in Fig. (8) in the absence of the magnetic field and Fig. (9) in the presence of the magnetic field. Also, the breakdown potential is decreased in the presence of the magnetic field, as shown in Fig. (10).

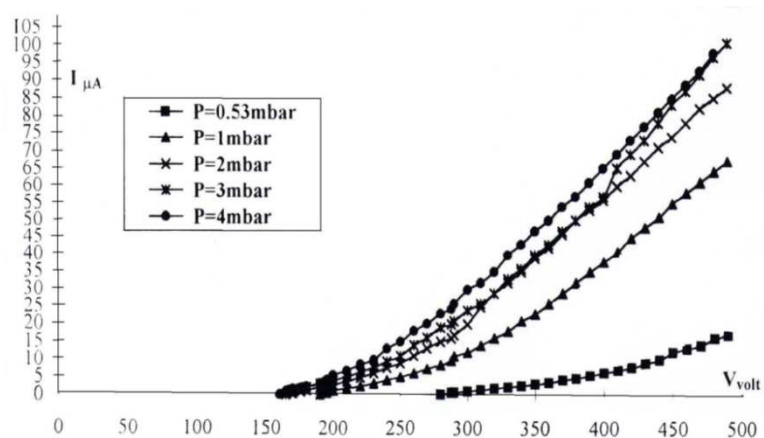


Fig. (8) The  $(I_a-V_a)$  characteristic curves of the Helium gas discharge at different pressures, when the distance between the two electrodes was fixed at (3.2 cm)

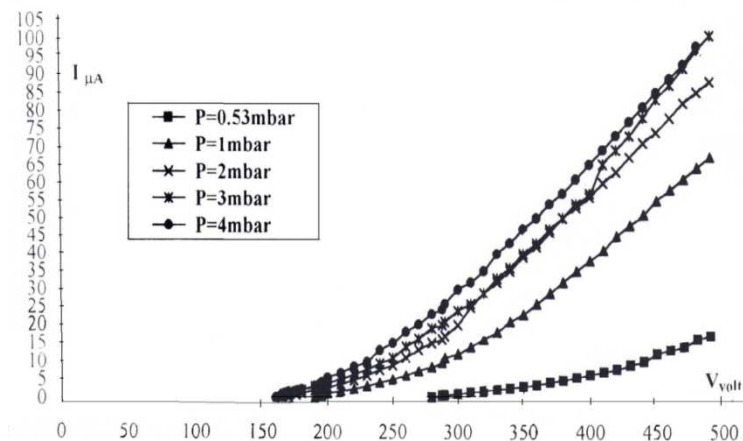


Fig. (9) The (Ia-Va) characteristic curves of Helium gas at different pressures when applied the external magnetic field

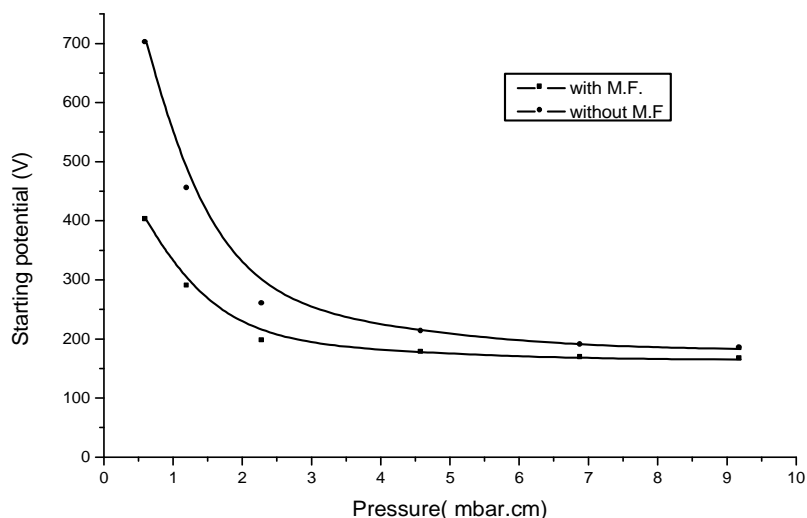
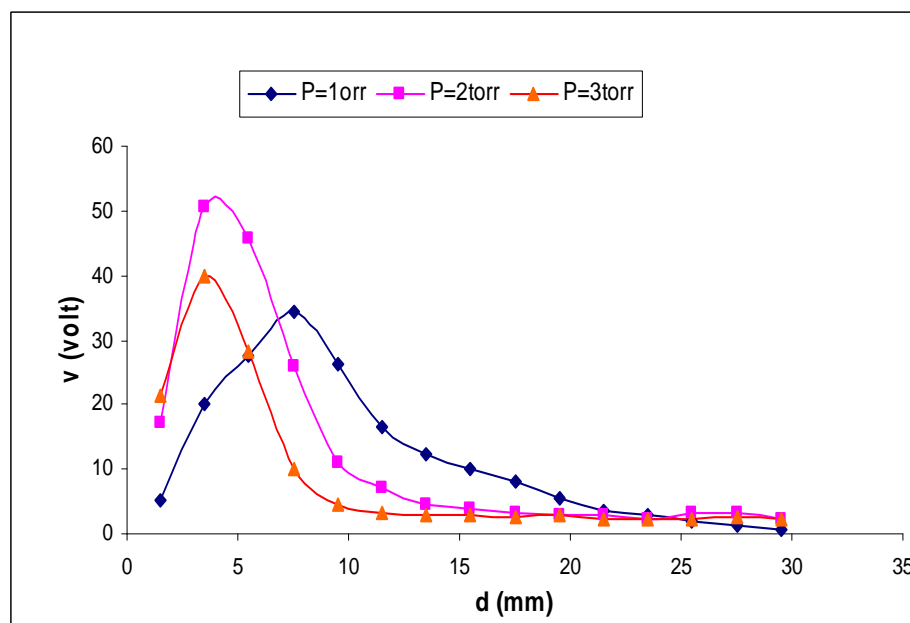


Fig. (10) The breakdown potentials measurements with and without the magnetic for the Helium gas at different pressures.

The factor of decreasing the breakdown potential for Helium is large than those in Argon which may be attributed to the larger ionization energy of Helium. Values of the current discharge in the presence of the magnetic field for Helium is larger than those in the absence of the field thus the slopes of the curves are larger (i.e. the resistance of the discharge is small in the presence of the magnetic field).

### 3-3. The CATHODE FATT THICKNESS MEASUREMENTS.

The axial potential distribution has been measured along the axis of the discharge tube using single probe; at different Ar gas pressure is shown in Fig. (11). The potential increases rapidly near the cathode until it reaches a maximum value at the end of cathode fall region, this rapid increase in potential can be referred to the existence of positive space charge within the cathode fall region. After the peak, the potential decreases less rapidly due to the existence of the reversal field in the negative glow and at the beginning of Faraday dark space (FDS) [10].



**Fig. (11) The axial potential distribution along the axis of the discharge tube using single probe at different Ar gas pressures.**

On the other hand, Fig. (12) shows the cathode fall thickness ( $X_c$ ) measurements with and without the magnetic field at different Ar gas pressure. It can be seen from Fig. (12) that the cathode fall thickness ( $X_c$ ) decreases with increasing in the gas pressure. The decreases in  $X_c$  as the gas pressure increases can be attributed to the increase in the ionizing collision frequency and hence the discharge needs less distance to create the negative glow region [3].

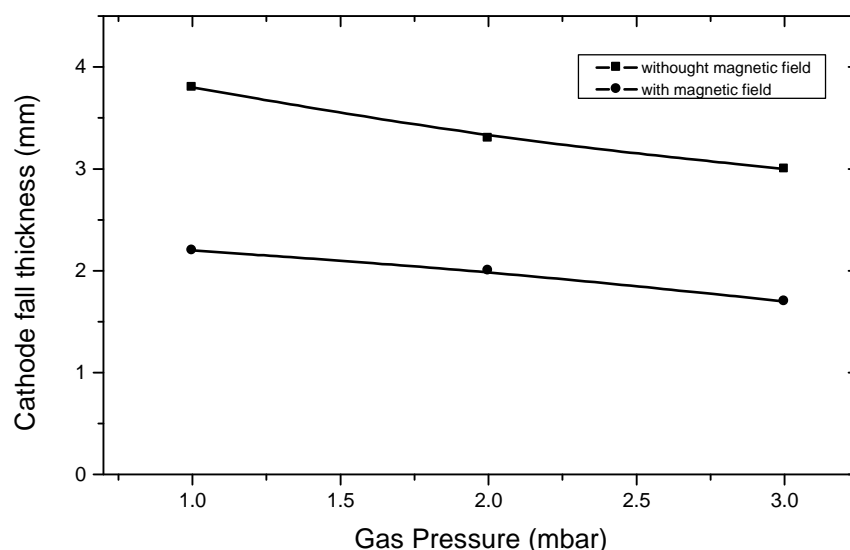


**Fig. (12) the cathode fall thickness measurements with and without the magnetic field at different Ar gas pressures**

When the magnetic field is applied, the cathode fall and negative glow regions are compressed, so higher values of potential are expected. It decreased the length of the cathode fall region ( $X_c$ ).

This effect is very powerful because electrons have beam – like properties in this region. This will of course increase the electric field in this region and thus ions would accelerate more and efficient sputtering would increase [11].

### CONCLUSION

Low-density plasma is generated in a cylindrical DC magnetron discharge tube. The distribution of the magnetic field strengths in the radial direction of the cathode electrode and the axial distribution between the two electrodes are drawn. Also, the ( $I_a$ - $V_a$ ) characteristic curves of the glow discharge have been measured for Ar and He gases with and without magnetic field.

Values of the discharge current in the presence of the magnetic field for Argon are smaller to those in the absence of the magnetic field. Thus, slopes of the ( $I_a$ - $V_a$ ) curves in the presence of the magnetic field are smaller than those in the absence of magnetic field.

Values of the current discharge in the presence of the magnetic field for Helium is larger than those in the absence of the field thus the slopes of the curves are larger.

The cathode fall thickness ( $X_c$ ) decreases with increasing in the gas pressure. When the magnetic field is applied, the cathode fall and negative glow regions are compressed, so higher values of potential are expected. It decreased the length of the cathode fall region.

### REFERANCES

- [1] Grill A, Cold Plasma in Material Fabrication from Fundamental to Applications, IEEE Press, **1993**.
- [2] Nasser E, Fundamental of Gaseous Ionization and Plasma Electronics, Wiley- Interscience, New York, **1971**.
- [3] Parke Ph, The Fundamentals Electronics of Gas Discharge Tubes, Chapter 15 in Electronics, Edward Arnold Pub, Ltd, **1963**.
- [4] Zou X, Liu JY, Gong Y, Wang ZX, Liu Y, Wang XG, **2004,73**, 681.
- [5] Farhad Masoudi S, **2007**,81, 871.
- [6] Liu JY, Zhao F, Zou X, Zhang Y, Liu Y, Wang XG, **2006**, 80, 1206.
- [7] Surzhikov S , *High Temperature*, **2009**,47, 459.
- [8] Auger M, Vazquez L, Jergel M, *Surf. Coat. Technol.*, **2004**, 180 , 140.
- [9] Bunshah, R, Deposition Technologies for Films and Coatings: Developments and Applications, Noyes Publications, *Park Ridge, NJ*, **1982**.
- [10] Kimura T, Kano A, Ohe K, *Phys. Plasma*, **1995**,2 ,4659.
- [11] Yuan Zhongcai, Shi Jiaming, Xu Bo , Ma Liu, *Plasma Sci. Technol.*, **2008**,10, 446.